Biol. Cybern. 72, 455–461 (1995)

Biological Cybernetics

Modulated excitability: a new way to obtain bursting neurons

Ehud Sivan[1,2], Lee Segel[3], Hanna Parnas[1,4]

[1] Department of Neurobiology, Institute of Life Sciences, Hebrew University, Jerusalem 91904, Israel
[2] Department of Computer Science, Hebrew University, Jerusalem 91904, Israel
[3] Department of Applied Mathematics and Computer Science, Weizmann Institute of Science, Rehovot 76100, Israel
[4] The Center for Neural Computation, Hebrew University, Jerusalem 91904, Israel

Received: 14 July 1994 / Accepted in revised form: 25 October 1994

Abstract. Classical burster models are based on a fast system that either oscillates or is quiescent, depending on temporarily fixed values of slow variables. In a study of the lobster heart ganglion, we found a new type of burster for which the fast system is globally stable for all relevant fixed values of the slow variables. We describe how this burster works and speculate on its biological significance.

1 Introduction

Bursting neurons exhibit periods of oscillation separated by periods of quiesence. We present here a bursting model of a new type, one that is centered on excitability rather than oscillation. We came upon the new type of burster in a study of biophysically motivated models for bursting cells in the cardiac ganglion of the lobster. This leads us to expect that the new type of burster might prove to be physiologically significant.

We begin with a mathematical perspective. (Later we shall take a more biophysical point of view.) Classical mathematical explanations of bursting behavior (see, for example, Rinzel and Lee 1987; Rinzel and Ermentrout 1989) consider situations in which variables can be divided into two categories, fast and slow. The first step is to examine the fast variables when the slow variables are held at fixed values and hence temporarily regarded as parameters. Depending on these parameters, two types of behavior are found. Typically, for some parameter values periodic oscillations are seen while for others the fast system always tends to a steady state. Bursting occurs when the slow parameters are allowed to vary according to their governing equations. If conditions are appropriate, oscillations in the fast variables move the slow variables out of the domain where fast oscillations occur (if the slow variables are temporarily fixed) and into the domain where the fast system is at steady state. At steady values of the fast variables, however, the slow variables ultimately move to the domain corresponding to fast oscillations. Bursting thus results from the alternating movement of the slow variables from the domain giving fast oscillation to the domain giving a steady state.

We came upon a new type of burster in efforts to build on the results of Av-Ron et al. (1991, 1993), who presented a basic biophysical model for bursting neurons. (From now on these papers will be referred to as I and II.) These papers constitute the first part of a study in neuronal modelling whose aim is to determine whether one can select different parameter values for the same basic model in such a way that when such model cells are linked into a suitably connected small network, then each individual cell would exhibit the bursting behavior observed by Friesen (1975a,b) in the lobster cardiac ganglion. This particular example is regarded as a test case for a general approach.

There are four bursting cells in the cardiac ganglion of the lobster, cells 6–9. After we arrived at specific candidate models for each of these, we began to examine them in the spirit of the classical bursting explanation. We found to our surprise that in our cell 9 model, the fast equations did not exhibit oscillation for any relevant fixed values of the slow variables. There was always a globally stable steady state. It therefore seems that our cell 9 burster is of a new type: in the absence of fast oscillations when the slow parameters are fixed, there seems no relevance to the classical explanation for bursting (slow variables move the fast system back and forth between oscillation and quiesence).

How could bursting possibly stem from such a stable system? Further examination of the equations gave a clue. When we kept the slow variables fixed at various relevant values, then the two fast equations form an excitable system. That is, even though all perturbations eventually died out, and the system inevitably returned to rest, there were important transient effects. Although relatively small perturbations to the steady state (the rest state) decayed monotonically, superthreshold perturbations fired an action potential after which the system indeed returned to rest. Perhaps when the slow variables are permitted to vary conditions can be such that the excitability threshold can be repeatedly crossed.

Following up on the surmise just stated, in this paper we explore the mechanisms by which bursting can result from superimposing suitable slow variation on a fast excitable

Correspondence to: L. Segel

system. We first examine how a sequence of spikes can indeed be generated from such a system, in spite of the fact that for the fast system a single triggered spike is expected to be followed by a return to rest. Once we explain how such a spike sequence can in principal be generated, we then solve the problem of why the sequence ceases – to produce the quiescent part of the cycle. Finally, we explain why the spikes start again. From a biophysical point of view, our reasoning rests on the phenomenon of anodal break excitation.

In our concluding discussion, we state why we think that the excitable burster is far more than an amusing curiosity and may actually play a central role in small neuronal networks.

2 The basic burster model

In this section we present a basic set of equations for modelling bursting neurons, with an eye to applying the model to lobster cardiac ganglion cells. For these same equations, but for two different sets of parameter values, we find two different types of bursters. The first burster is fairly conventional, but the second is novel.

The fundamental equation equates the capacitive current (with capacitance C_m) to the sum of an applied current I_{app} introduced by the experimenter and the total ionic current I_{tot}:

$$C_m dV/dt = I_{app} - I_{tot} \tag{1}$$

The sodium, potassium and leak currents of the classical Hodgkin-Huxley model are supplemented by a calcium-dependent potassium current and a calcium current:

$$I_{tot} = I_{Na}(V,W)+I_K(V,W)+I_L(V)+I_{K(Ca)}(V,C)+I_{Ca}(V,X) \tag{2}$$

In describing the currents, we follow a standard approximation scheme; see Rinzel (1984). Also see I. Thus

$$I_{Na}(V,W) = \bar{g}_{Na} m_\infty^3(V)(1-W)(V-V_{Na}), \tag{3}$$

$$I_K(V,W) = \bar{g}_K (W/s)^4 (V-V_K), \tag{4}$$

$$I_L(V) = \bar{g}_L (V-V_L). \tag{5}$$

In (3–5) $\bar{g}_{Na}$, $\bar{g}_K$, $\bar{g}_L$ stand for maximal ionic conductances, while V_{Na}, V_K, V_L, denote the reversal potentials of the corresponding currents. In (3), the steady state sodium activation gate, $m_\infty(V)$, is described by a general sigmoid function

$$F_\infty(V;a,V_{1/2}) = \frac{1}{1+e^{-2a(V-V_{1/2})}} \tag{6}$$

where a controls the sigmoid's steepness and $V_{1/2}$ its midpoint. In this case

$$m_\infty(V) = F_\infty(V;a_m,V_m) \tag{7}$$

The recovery variable W is described by

$$\frac{dW}{dt} = \frac{W_\infty(V)-W}{\tau(V)} \tag{8}$$

where the steady state value $W_\infty(V)$ has a sigmoidal dependence on voltage,

$$W_\infty(V) = F_\infty(V;a_W,V_W) \tag{9}$$

and the relaxation time of recovery $\tau(V)$ is given by

$$\tau(V) = \frac{1}{\lambda[e^{a_W(V-V_W)}+e^{-a_W(V-V_W)}]} \tag{10}$$

This expression for $\tau(V)$ is based on the assumption that W follows first-order kinetics for the transition from an active to an inactive state.

The two additional currents in (2) [i.e. $I_{Ca}(V,X)$ and $I_{K(Ca)}(V,C)$] are described somewhat differently from the classical ones. The calcium current was shown to exhibit saturative dependence on extracellular Ca^{2+} concentration, even at low concentrations (Hagiwara and Takahashi 1967; Akaike et al. 1978). As is conventional we describe $I_{Ca}(V,X)$ by the product of membrane conductance and the ion driving force:

$$I_{Ca}(V,X) = \bar{g}_{Ca} X \cdot V_{Ca}(V) \tag{11}$$

Here membrane conductance is accounted for by $\bar{g}_{Ca}$, the maximal calcium conductance, and X , the fraction of open calcium channels. To capture saturation, we replace the conventional driving force by

$$V_{Ca}(V) = \frac{\bar{V}_{Ca} Ce}{Ce + Ke \cdot Ke_\infty(V)} \tag{12}$$

where $\bar{V}_{Ca}$ is the maximal possible driving force, and Ce is the external calcium concentration. The term $Ke_\infty(V)$ is a sigmoid function of V, given as

$$Ke_\infty(V) = F_\infty(V;a_{Ke},V_{Ke}) \tag{13}$$

$Ke_\infty(V)$ increases with depolarization and represents the decreasing permeability of the channels to inward movements of calcium as membrane depolarization increases. The combined dependence of X and $Ke_\infty(V)$ on the membrane potential generates the experimentally observed bell-shaped dependence of I_{Ca} on V (Llinas et al. 1981). Accordingly, X saturates at higher depolarizations, whereas $Ke_\infty(V)$ continues to rise. As a result, I_{Ca} first rises owing to an increase in X, but then declines owing to a saturation of X and increasing $Ke_\infty(V)$. (For detailed discussion see Parnas and Segel, 1989.)

The third differential equation in the model describes the time course of X:

$$\frac{dX}{dt} = \frac{X_\infty(V)-X}{\tau_X} \tag{14}$$

Here $X_\infty(V)$ stands for the fraction of open channels at steady state, and is described by the sigmoid curve

$$X_\infty(V) = F_\infty(V;a_X,V_X) \tag{15}$$

The last current considered in the model, $I_{K(Ca)}(V,C)$, describes a potassium channel that is activated in a saturative manner by intracellular calcium, C. Thus,

$$I_{K(Ca)}(V,C) = \bar{g}_{K(Ca)} \frac{C}{K_d + C}(V-V_K) \tag{16}$$

Our final equation describes the temporal distribution of the intracellular calcium concentration. The calcium concentration rises due to voltage dependent influx of calcium and declines due to lumped removal processes:

$$\frac{dC}{dt} = Y_{Ca}(-I_{Ca}(V, X)) - R\frac{C}{C + K_r} \tag{17}$$

Here, R stands for the maximal rate of removal and K_r for the corresponding half-saturation constant.

In modelling the cardiac ganglion, we wish to demonstrate that all the ganglion cells can be described by (1)–(17), with different cell types corresponding to different parameter choices. This is not the place for a detailed discussion of this matter. For our present purposes, we wish only to present two cell types, with their accompanying parameter sets. These are found in Fig. 1. In accord with Friesen (1975a), our model for cell 6 has a burst duration of approximately 0.4 s with a frequency of 50 impulses per second; the bursting duration of cell 9 is about 1 s, with a frequency of 25 impulses per second.

Our basic model for bursting consists of four differential equations (1), (8), (14) and (17) for the dependent variables V, W, X, and C. Of these, the first two are fast, with intrinsic time scales of milliseconds. The last two are slow, with intrinsic time scales, respectively, of tens and hundreds of milliseconds. Thus, to unravel the mechanism of bursting, we should be able to perform the standard simplification of examining the V-W phase plane for various fixed values of the slowly changing variables C and X. When this was done for the model of cell 6 it was found that, in essence, there was precisely one attractor, either a stable steady state or a stable oscillation. (For our particular model of cell 6, there is a narrow parameter range at the beginning of the burst where there are 3 steady states; this does not modify our line of argument.)

Most bursting models are based on bistable fast dynamics, but essentially no bistability was found in our model for cell 6. We now briefly discuss some implications of the absence of bistability.

It can be shown that a single slow equation does not suffice to give bursting if the fast equations always have a unique attractor, as in the situation here. Suppose for definiteness that the attractor is an oscillator for relatively small values of the single slow variable. (This is the case in the present model if X is temporarily held fixed.) Suppose further that when the fast variables oscillate, the slow variable (C in the present case) increases beyond the appropriate threshold so that the sole attractor is now a steady state. This corresponds to the quiescent state of the burst. If the slow variable decreases when the fast variables are quiescent, then the threshold will be crossed again, and oscillations will recommence. But to have the possibility of independently regulating the length of the burst and the length of the quiescent period, there must be a way to keep the slow variable decreasing (increasing) after it has decreased (increased) past the oscillation-quiesence threshold. In particular, without such *persistence* (*inertia* is another good term) it is likely that the burst will consist of only a single spike.

Analogy with the spring equation in mechanics correctly suggests that a first-order equation for the slow variable

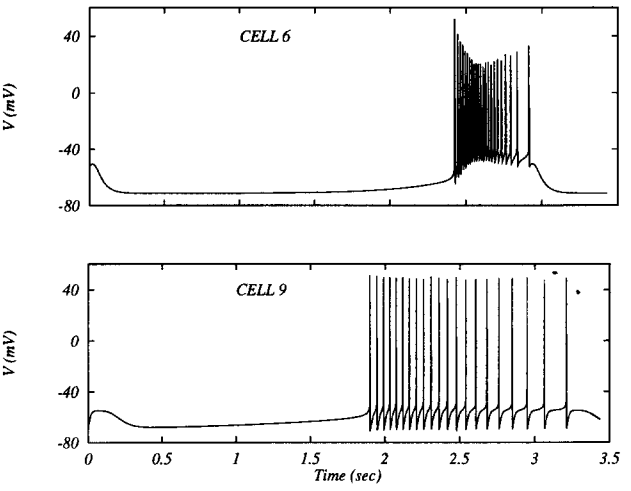

Fig. 1. Bursting behavior of model cells, 6 and 9. Graphs were obtained by numerically solving the model equations of system (1)–(17) by means of fourth-order Runge-Kutta methods. Parameters for cell 6: $C_m = 1\,\mu F/cm^2$, $\bar{g}_{Na} = 100$, $V_{Na} = 55$, $V_K = -72$, $s = 1$, $\bar{g}_L = 0.3$, $V_L = -60$, $a_m = 0.055$, $V_m = -30$, $a_W = 0.045$, $V_W = -47$, $\lambda = 0.02$, $\bar{V}_{Ca} = -180$, $C_e = 10\,\mu M$, $K_e = 100$, $a_{Ke} = 0.04$, $V_{Ke} = 60$, $a_X = 0.18$, $V_X = -50$, $\tau_X = 50\,ms$, $K_d = 0.5\,\mu M$, $K_r = 0.5\,\mu M$, $Y_{Ca} = 0.00002\,M/\mu A \cdot ms$, $\bar{g}_{K(Ca)} = 11$, $\bar{g}_K = 8$, $\bar{g}_{Ca} = 1.7$, $R = 0.00195\,\mu M/ms$. Cell 9: same as for cell 6, except that $\bar{g}_{K(Ca)} = 1.9$, $\bar{g}_K = 50$, $\bar{g}_{Ca} = 0.86$, $R = 0.001\,\mu M/ms$. Units: conductances (mS/cm^2), voltages (mV)

does not exhibit inertia, but that a second-order equation, or equivalently a pair of first-order equations, will supply inertia. Another way to express the same thought is that a pair of suitable equations for the slow variables, but not a single equation, can provide appropriate semi-autonomous oscillations of these variables that move the fast system between quiescence and oscillation in a controllable way. Indeed here, as is shown in Fig. 2A, when all four differential equations are simultaneously solved, the slow variables move in a circuit that brings them alternately in and out of the domain where the fast variables oscillate.

Often, the fast variables exhibit bistability for sets of fixed slow variables: quiescent and oscillating attractors coexist. Then "inertia" is supplied by hysteresis (Av-Ron et al, 1993).

Returning now to our main line of argument, we note that in sharp contrast to the situation for cell 6, for cell 9 the $V - W$ plane contains a single stable steady state for all fixed values of C and X that are encountered during the burst. To be precise, Fig. 2B shows that when the full set of equations (1)–(17) is solved, the values of C and X for cell 9 slowly cycle, as do those of cell 6. Suppose, however, that C and X are frozen at a point on this cycle; in no case will oscillations occur in the fast system for cell 9. In addition, note that for certain parameter ranges, there are intermediate cases for which a portion of the spikes does correspond to oscillations in the frozen fast system, but a portion does not. Our models for cells 7 and 8 are of this intermediate type (not shown), and even for cell 6, we see from Fig. 2A that the last two spikes occur in a stable region of the slow system.

The contrast between Figs. 2A and B exemplifies our central question: How can there be bursting when the frozen

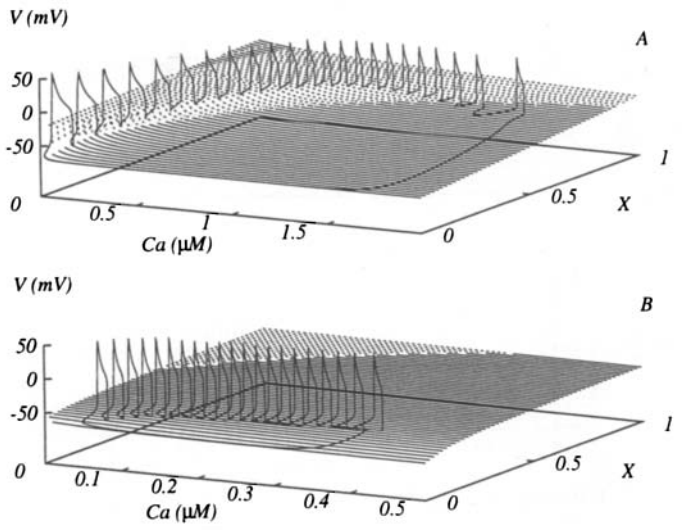

Fig. 2A,B. Trajectory of (C, X, V) for model cells. Below the trajectory is a plane each point of which describes the stability of the fast system if C and X are frozen at their instantaneous values. The plane is *dashed* or *solid* depending on whether the steady state is unstable or stable. **A** Model cell 6. As expected, the oscillations take place when the trajectory is in the unstable domain of the plane. (The last two spikes are an exception; see text.) **B** Model cell 9. Contrary to expectation, even during oscillations the projected trajectory is in the stable domain of the plane

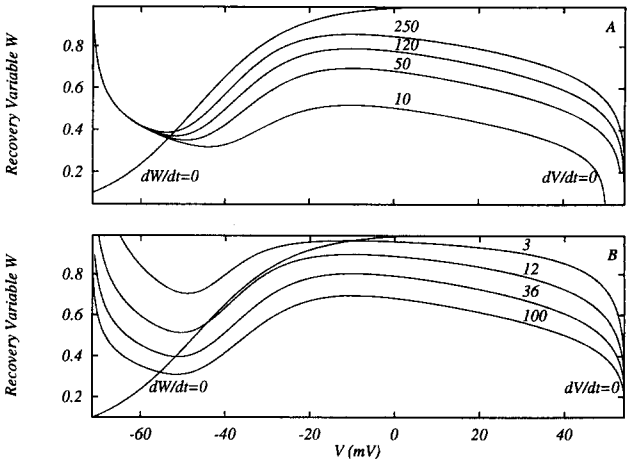

Fig. 3. Effects of changing sodium conductance (**A**) and potassium conductance (**B**) on the nullclines of the "fast" model with $C = 0.046209\,\mu$M, $X = 0.127971\,\mu$M. Other parameters as in our model for cell 9

fast system always seems to have a tendency to head toward a stable rest state? We now begin our answer to this question.

3 Behavior of the fast system

As we have pointed out, the classical path to understanding bursting begins with an examination of the fast $V - W$ subsystem for fixed C and X. Here this system is composed of differential equations (1) and (8) for V and W, wherein the calcium-dependent potassium current and the calcium current now depend solely on voltage. It is helpful to think of the remaining voltage-dependent currents (sodium and potassium) as representative depolarizing and hyperpolarizing agents, for this will be seen to be the key to exploiting the findings we make upon examining the fast submodel.

We depict in Fig. 3 results concerning the effect of varying, respectively, the sodium and potassium conductivities on the nullclines of the differential equations (1) for V and (8) for W. For present purposes, the following observations are noteworthy. (i) The nullclines, and hence the behavior of the model, are considerably more sensitive to variations in the potassium conductance than they are to sodium conductance. (ii) The nullclines intersect once, so that there is a single steady-state point. (iii) As is well known, the steady-state point is unstable if the intersection is on the rising portion of the V nullcline, except very near the ends. The steady state is stable if it is on the falling portions of the V nullcline. When a stable steady state is near the minimum of the nullcline, excitability is found. (Results (i)–(iii) also hold for the parameters employed in I.) (iv) For our particular model, with "standard" parameter values, it is found that stable oscillations exist when the steady state is unstable, and in particular for potassium conductances that range from 5 to $20\,\mathrm{mS/cm^2}$.

As a first application of the findings summarized in Fig. 3, we note from Fig. 3B that the rest state is globally stable for potassium conductances greater than about $40\,\mathrm{mS/cm^2}$. In the cell 9 model of Fig. 1B, the potassium conductance is $50\,\mathrm{mS/cm^2}$. The effective potassium conductance is even larger, because of the additional presence of the calcium-dependent potassium channel. We thus return again from a slightly different point of view to the challenge with which we concluded the previous section, how can we possibly obtain bursting with this strong tendency of the system to return to rest?

4 The second spike: anodal break excitation

In analyzing the mechanism for the new burster, we start with the following question. Suppose that somehow a spike is initiated; why should a second spike appear? Answering this question will require us to review the well-known phenomenon of anodal break excitation (FitzHugh 1961).

Figure 4A depicts the phase plane of the fast variables V and W when C and X are fixed at the values they attain just after the first spike in the burst. Let us first examine this figure in isolation, as a particular example of $V - W$ dynamics given by the differential equations (1) for $\mathrm{d}V/\mathrm{d}t$, with the applied current I_{app} equal to zero, and (8) for $\mathrm{d}W/\mathrm{d}t$. For the moment, let us disregard the fixed slow variables and the role that their modification plays in the burst.

In the phase plane of Fig. 4A, there is a single stable steady state, denoted by a circle. Indeed whatever the initial conditions, the solution eventually tends permanently to this rest state. The heavy dashed line delineates an excitability threshold. If initial conditions are above and to the left of this line, solutions tend to the rest state without a tendency for an overall voltage increase. As shown by trajectory T_1, for example, even if the voltage initially exceeds rest there is a rapid decrease at constant W, followed by a slow shift

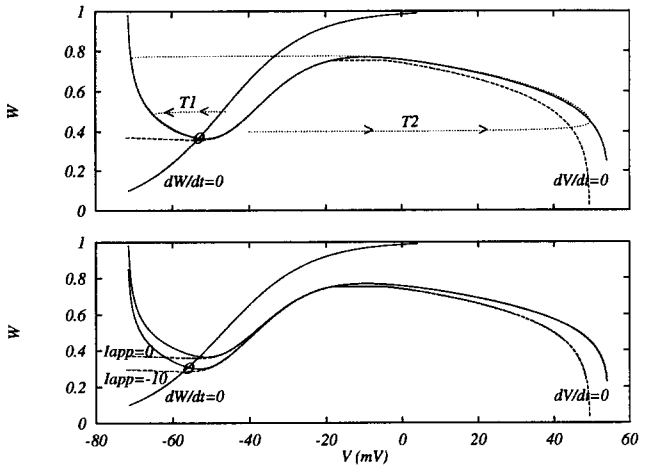

Fig. 4A,B. Thresholds in the fast ($V - W$) phase plane. (Here and below, graphs are all for cell 9.) The slow variables are fixed at their values just after the first spike in the burst. See Fig. 3 for exact values. **A** *Solid lines* denote the V and W nullclines, while the *circle* represents the stable steady state. A threshold (*dashed line*) divides the plane into excitable and nonexcitable regions – as is illustrated by the trajectories T_1 and T_2. **B** The effect of a hyperpolarizing applied current ($I_{app} = -10\,\mu A/cm^2$) on the steady state (circle) and threshold

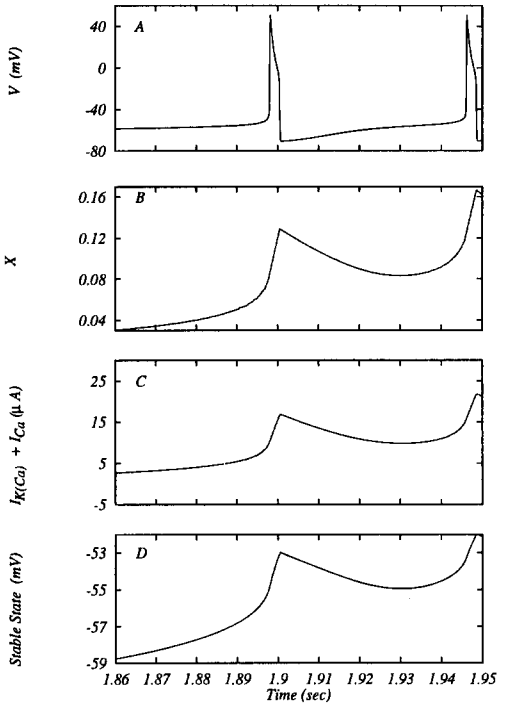

Fig. 5A–D. Dynamics between the first and second spikes of the burst. **A** Membrane potential V. **B** Voltage-dependent activation variable X of the calcium channel. **C** Sum of the inward Ca^{2+} current, I_{Ca}, and the outward calcium-dependent potassium current $I_{K(Ca)}$. (*Positive values* indicate inward current.) **D** Instantaneous rest voltage, i.e., that given by the stable steady state of the fast system with C and X fixed at the values that they take at the given time

of V and W to their rest values. But if initial conditions are such that V and W start below and to the right of the heavy dashed line (e.g., trajectory T_2) the corresponding solutions first move rapidly to the right, tracing an action potential, before they return to rest.

To demonstrate anodal break excitation let us alter the situation in Fig. 4A by instantaneously adding a fixed hyperpolarizing current. Then I_{app} in (1) instantaneously shifts from zero to a fixed negative value. As a consequence, the V nullcline instantaneously drops vertically by an amount $|I_{app}|$, yielding in particular a new rest state at lower values of V and W. (The system will take some time to attain this new stable rest state.) Because the new steady state is lower (circle), the threshold is also lowered (Fig. 4B). Whenever the hyperpolarizing current is turned off, the original stable steady state and threshold are immediately regained. But if the hyperpolarizing current had been maintained for a sufficiently long time, V and W would have moved close to the steady state that is appropriate for hyperpolarized conditions. As a result, when the original stable steady state is regained, V and W will be in a superthreshold condition, and an action potential will be fired.

We wish to demonstrate that a phenomenon similar to the anodal break excitation is responsible for the formation of the second spike in our burster. We will show that the changes in C and X provide an effective anodal break excitation – *not* in a direct manner via a temporary *externally applied* hyperpolarizing current, but rather by a temporary *internally generated* hyperpolarizing effect.

In our model, C and X affect V and W via the currents I_{Ca} and $I_{K(Ca)}$. Therefore, we focus on the behavior of these two currents. We call these currents *controllable*, for while all currents are, of course, voltage-dependent, only these have additional modulatory factors.

At the end of the first spike, the membrane potential is strongly hyperpolarized (see Fig. 5A, time = 1.9 s). Since X is still high (Fig. 5B), I_{Ca} dominates over $I_{K(Ca)}$, and these two opposing currents result in a net inward contribution of the controllable currents (Fig. 5C). Upon gradual membrane repolarization (Fig. 5A), the net inward contribution declines (Fig. 5C). Consequently, the V nullcline shifts downward. At the same time, X declines from its maximal value, which is attained at the peak of the spike. But since V increases during that same time (Fig. 5A), X eventually starts to increase again (Fig. 5B, $t = 1.93$ s). Consequently there is a rise in I_{Ca}, which results in a higher net inward contribution from I_{Ca} and $I_{K(Ca)}$ and hence in an upward shift of the V nullcline at $t = 1.93$ s (Fig. 5C).

Figure 5D shows the voltage at the instantaneous (stable) steady state point of the $V - W$ subsystem. This point is the intersection of the V and W nullclines, and the latter is unchanged throughout the burst. Thus, the shifts up and down of the V nullcline parallel the shifts in the stable-state point that are seen in Fig. 5D.

The time up to the new rise in this net inward contribution of the controllable currents is analogous to the time of administering hyperpolarizing external current in the anodal break excitation. Furthermore, the rise in the net inward controllable current corresponds to the cessation of this hyperpolarizing current. Similarly to anodal break excitation, shortly after the rise commences V and W enter the excitable domain.

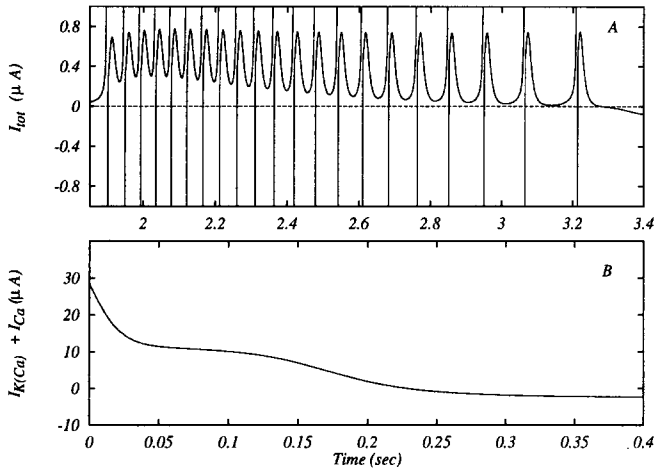

Fig. 6. **A** The sum of all the currents, during a burst, from (2). The *nearly vertical lines* denote the "off-scale" behavior during the spikes. Between spikes, inward current dominates until the last spike is fired, after which a net outward current takes over. **B** The control current after the last spike

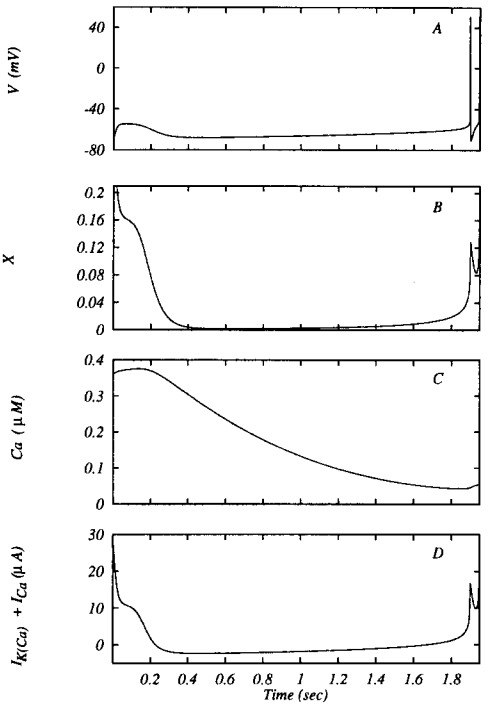

Fig. 7. Dynamics during the quiescent period and the first spike

In classical anodal break excitation, discontinuities in applied hyperpolarizing current bring about virtually instantaneous corresponding jumps in the V nullcline (Fig. 4). Here the amount of hyperpolarization changes smoothly but relatively rapidly. The motion of the V nullcline is such that the actual state (V, W) of the fast system lags in its chase of the instantaneous steady state in such a way that after a time superthreshold conditions result. (In the simulations of Fig. 5 the threshold is crossed at $t = 1.944$.) Repeated lags result in repeated spikes of the burst.

5 Why the burst stops and why it starts again

We have seen how an effective anodal break excitation is responsible for the generation of a second spike, given that a first spike has somehow been triggered. Why is there not an indefinite repetition of this process, generating an infinite train of spikes? The answer is that there is net calcium entry during the spikes. The build up of calcium eventually increases the calcium dependent potassium conductance so much that the increased potassium outflow leads to a dominance of outward current (Fig. 6A). There is such a weakening of the repolarization phase of the effective anodal break excitation that eventually an additional spike is not generated. This is the beginning of the quiescent phase of the burst.

Figure 6B provides further understanding of the difference in behavior between successive spikes on the one hand, and after the last spike on the other. In contrast to Fig. 5C, comparison of Fig. 6B and Fig. 5C shows that after the last spike, the net inward controllable current declines continuously, so that the "cessation" of the hyperpolarizing effect does not occur.

During quiesence, the dominance of outward current leads to a drop in voltage (Fig. 7A), and hence to a decrease in X (Fig. 7B), in calcium concentration (Fig. 7C), and in the total controllable current $I_{K(Ca)} + I_{Ca}$. After some time, the intracellular calcium concentration drops so far and the calcium-dependent potassium current consequently becomes so low that inward current dominates. Now voltage begins slowly to rise, with a concommitant increase in X and C (Fig. 7). Eventually, the anodal break threshold is crossed, and the first spike of a new burst is generated.

6 Discussion

We stumbled upon a new type of bursting in the course of modeling the lobster cardiac ganglion. The novel nature of the burst is revealed by the well-known procedure of exploiting the fact that two dependent variables (the voltage V and the recovery variable W) change on a time scale that is much shorter than that of the other two (the calcium concentration C and its gating variable X). In the case of interest, the full set of four differential equations has no stable steady state; the burst is an oscillatory attractor. By contrast, for relevant fixed values of C and X the fast $V-W$ equations always have a globally attracting stable steady state. For burster models studied heretofore, one would expect the fast equations to have an oscillatory attractor for certain ranges of C and X. Without such an attractor, it would appear that there would be no way that changes in C and X could generate the train of voltage spikes that constitute the active phase of the burst. Nonetheless, we show that such a train indeed can be generated, by a mechanism closely related to anodal break excitation.

The model excitable burster and the corresponding biological excitable burster show great similarity in behavior. This suggests that the new type of burster might have biological relevance.

To appreciate the possible role of this new type of burster, we briefly summarize some relevant properties of our model of the lobster cardiac ganglion. The control portion of the ganglion consists of four bursting cells of which one, cell 6, was shown in Fig. 2A to exhibit classical bursting behavior. Another, cell 9, exhibits the new excitable type of bursting. The other two cells, 7 and 8, display intermediate behavior (not shown).

Sivan et al. (1994, manuscript submitted) investigated the sensitivity of model cells 6 and 9 to an applied current whose duration was a few milliseconds. They examined several types of response and always found the same general conclusion: cell 9 is very much more easily disturbed than cell 6. To give one example, they tested for the magnitude of current that would stimulate a premature burst. In both cases, this was only possible in the latter third of the quiescent period. For cell 9, a puff of current was sufficient, approximately 10 nA/cm^2. For cell 6, about twenty times as much current was required, a magnitude that is unlikely to occur under physiological conditions.

Recall that cells 7 and 8 are intermediate in their properties between cell 6 and cell 9. Thus, the controlling cells of our model cardiac ganglion range from one that is hardly responsive to the external environment (cell 6) to one that is extremely sensitive (cell 9, the excitable burster). Together, these four model cells form a unit that simultaneously fulfills two superficially contradictory requirements. The unit may be able to perform adequately in the face of the malfunctioning or death of one of its cells, or in the face of an inappropriate input. But this robustness is not at the price of a complete lack of sensitivity. Especially by virtue of cell 9, the unit can alter its behavior in response to external signals that aim to modulate cardiac output.

The different mechanisms of bursting are fully in accord with the different behaviors of cells 6 and 9. Cell 6 has a mind of its own. Except in transition stages, its fast system knows what it wants to do – either oscillate or be quiescent. By contrast, cell 9 is always sensitive to perturbation, for cell 9's fast system is always near the border between oscillation and quiesence. It could well be of significance that this representative model ganglion is controlled by a linked group of cells whose individual behavior ranges from imperturbable to excitable.

Acknowledgement. Thanks to G. de Vries for valuable comments on an earlier version of the manuscript.

Note added in proof: In Figs. 5C, 6B and 7D, the control current at time t is calculated using the steady state voltage at that time. This approximate control current is a good analog of I_{app} in an anodal break excitation.

References

Akaike N, Lee KS, Brown AM (1978) The calcium current of the *Helix* neuron. J Gen Physiol 71: 509–531

Av-Ron E, Parnas H, Segel LA (1991) A minimal biophysical model for an excitable and oscillatory neuron. Biol Cybern 65:487–500

Av-Ron E, Parnas H, Segel LA (1993) A basic biophysical model for bursting neurons. Biol Cybern 69:87–95

FitzHugh R (1961) Impulses and physiological states in models of nerve membrane. Biophys J 1:445–466

Friesen WO (1975a) Physiological anatomy and burst pattern in the cardiac ganglion of the spiny lobster *Panulirus interruptus*. J Comp Physiol 101:173–189

Friesen WO (1975b) Synaptic interactions in the cardiac ganglion of the spiny lobster *Panulirus interruptus*. J Comp Physiol 101:191–205

Hagiwara S, Takahashi K (1967) Surface density of calcium ions and calcium spikes in the barnacle muscle fiber membrane. J Gen Physiol 50:583–601

Llinas R, Steinberg IZ, Walton K (1981) Relationship between presynaptic calcium current and postsynaptic potentiation in squid synapse. Biophys J 33:322–351

Parnas H, Segel LA (1989) Facilitation as a tool to study the entry of calcium and the mechanism of neurotransmitter release. Prog Neur 32:1–9

Rinzel J (1984) Excitation dynamics: insights from simplified membrane models. 68th annual meeting of the Fed Am Soc Exp Bio, St. Louis

Rinzel J, Ermentrout GB (1989) Analysis of neural excitability and oscillations. In: Koch C, Segev I (eds) Methods in neuronal modeling: from synapses to networks. MIT Press, Bradford

Rinzel J, Lee YS (1987) Dissection of a model for neuronal parabolic bursting. J Math Biol 25:653–675